Short Communication Wiley Online Library

ELECTROANALYSIS

DOI: 10.1002/elan.202060308

# Label-free Selective Detection of Protein Markers in the Picomolar Range Via a Convenient Voltammetric Sensing Strategy

Chun-Yu Chen[a] and Joshua Lehr*[a, b]

**Abstract:** A convenient strategy for the preparation of label-free selective protein biomarker sensors is presented. After formation of a ferrocene terminated monolayer on a gold electrode using thiol chemistry, grafting of an antifouling phenylalanine layer onto the preformed ferrocene monolayer is achieved by diazonium chemistry. This provides a platform for receptor (anti-BSA or anti-CRP) immobilization as well an antifouling interface. Specific target binding leads to attenuation of the voltammetric faradaic signal of the underlying ferrocene group. Thereby, label-free, selective, voltammetric detection is achieved with highly competitive limits of detection in the low ($\leq 4$) picomolar range for both BSA and CRP.

**Keywords:** biosensor · label-free · ferrocene · biomarker

The sensitive detection of specific protein biomarkers is vital in the diagnosis of a range of medical conditions [1]. Traditional methods of protein biomarker detection, such as enzyme-linked immunosorbent assays (ELISA), while highly sensitive and selective, suffer from significant drawbacks, being high-cost multistep procedures which are carried out by technicians off-site. Consequently, there has been significant interest in the development of sensors for rapid, low-cost, on-site detection. Biosensors employing a range of transduction methodologies (optical [2], nanomechanical [3], and electrochemical [4], etc) have been investigated. Electrochemical sensing is particularly attractive being fast, sensitive, and easily integrated into existing electronics for convenient readout.

Traditionally, electrochemical protein/biomarker detection has been achieved by the addition of a redox-active species to the analyte solution, whose electrochemistry is attenuated by selective target binding to a receptor-functionalized electrode interface [5]. While sensitive, the requirement of adding a redox species to the sampling solution limits the practical applicability of this "faradaic" approach. Further work has focused on the development of truly "label-free" sensing methodologies. Such strategies include detecting target binding by probing subtle changes in the non-faradaic properties of the electrode interface [6] or by incorporating redox-active species into the surface sensing architecture, whose electrochemical signature changes upon target binding [7]. In both cases detection has generally been achieved by involved impedimetric analysis.

Herein we report on a simple, versatile route to redox-active selective sensing interfaces and demonstrate their application to the label-free voltammetric quantification of picomolar concentrations of specific target proteins. The strategy (Scheme 1) consists of grafting phenylalanine onto a preformed ferrocenethiol molecular monolayer on a gold electrode using diazonium chemistry. Diazonium chemistry has been previously employed in the fabrication of biosensors [8]. The phenylalanine moieties serve as sites for receptor/antibody immobilisation while having also been shown to demonstrate antifouling properties [9], thereby facilitating selective sensing. Coupling of an antibody onto the phenylalanine terminated film yields a selective, ferrocene-incorporating, protein-receptive electrode interface. Target quantification is achieved (in the picomolar range) by recording changes in the voltammetric charge associated with the ferrocene/ferrocenium ($Fc/Fc^+$) redox couple upon exposure of the electrode to the specific target protein. The strategy is demonstrated with two antibody/antigen conjugates: (anti-) bovine serum albumin (BSA) and (anti-) C-reactive protein (CRP). The former is widely available with a well understood reactivity, while the latter is a biomarker for inflammation, cancer, and cardiovascular disease, in humans. The present strategy provides a straight-forward route for the

[a] C.-Y. Chen, J. Lehr
Department of Chemistry & Forensics, Nottingham Trent University, Clifton Lane, Clifton, Nottingham, NG11 8NS, United Kingdom
[b] J. Lehr
School of Science, Engineering and Environment, University of Salford, 43 Crescent, Salford, M5 4WT, United Kingdom
E-mail: j.lehr@salford.ac.uk

Supporting information for this article is available on the WWW under https://doi.org/10.1002/elan.202060308

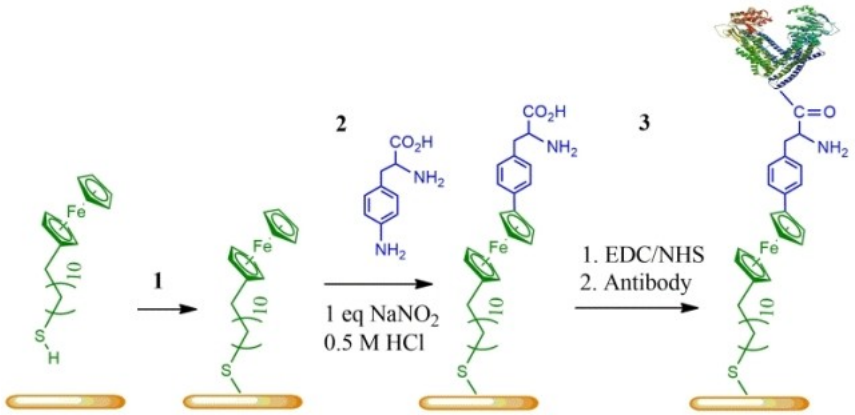


Scheme 1. Preparation of the sensing interface reported herein. Step 1: formation of the ferrocenethiol monolayer on a gold electrode. Step 2: grafting of amino-DL-phenylalanine onto the ferrocenethiol primer layer via in-situ formation of the corresponding diazonium cation. Step 3: Coupling of the receptive antibody onto the film.

preparation of redox-active sensing molecular layers, which does not require the extensive presynthesis of film components of previously reported strategies, while offering comparable (if not superior) sensitivities employing voltammetric, as opposed to more time consuming impedimetric, techniques.

Construction of the sensing interfaces was monitored by evaluating the redox response of the surface bound ferrocene. Cyclic voltammograms were recorded in blank electrolyte after each step of the film construction. After immersion of the bare gold electrodes in 11-ferrocenylundecanethiol solution, cyclic voltammograms (Figure 1) revealed the expected $Fc/Fc^+$ redox couple indicating the successful formation of a ferrocenethiol layer on the electrode surface (Scheme 1, step 1). A linear relationship between the scan rate and the peak current (Figure 1, insert) further confirms the ferrocene groups are surface bound. The ferrocenethiol layers proved highly stable to electrochemical cycling with only negligible changes in the magnitude of the $Fc/Fc^+$ redox signal over hundreds of cycles (in aqueous electrolyte). Integration of the voltammetric charges yielded surface concentrations of electroactive ferrocene groups in the range of $4.3–4.9\times10^{-10}$ mol cm$^{-2}$ for these films, in line with previous experimental reports and theoretical expectations for ferrocenethiol monolayers at gold interfaces [10].

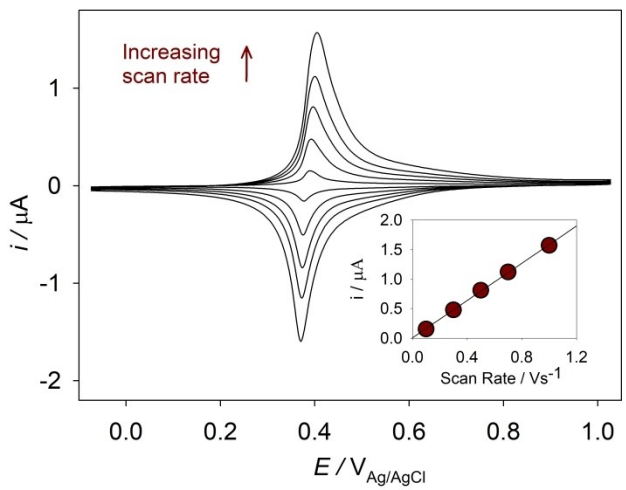


Fig. 1. Cyclic voltammetric scans of a gold working electrode after formation of ferrocenethiol film, recorded in 0.2 M $NaClO_4$ at scan rates of 0.1, 0.3, 0.5, 0.7, and 1.0 $Vs^{-1}$. Insert: plot of scan rate vs. oxidation peak current ($R^2=0.9995$) – the linear relationship confirms the ferrocene is surface bound.

After immersion of the ferrocene-modified electrode in a solution of amino-DL-phenylalanine and $NaNO_2$ in 0.5 M HCl, the surface concentration of electroactive ferrocene groups was seen to decrease to $1.2–1.5\times10^{-10}$ mol cm$^{-2}$ consistent with the formation of a blocking phenylalanine film bound to the ferrocene monolayer (SI 1). Aryl amines are known to form in-situ generated diazonium cations in the presence of $NaNO_2$ in HCl [11]. The diazonium species may be reduced to an aryl radical by a ferrocene moiety to which it subsequently couples covalently via the Gomberg-Bachmann reaction (Scheme 1, step 2) [12]. In addition to the decrease in electroactive ferrocene groups observed upon phenylalanine grafting, a cathodic potential shift of the $Fc/Fc^+$ redox couple from $E_{1/2}\approx0.383$ to $E_{1/2}\approx0.334$ vs. Ag/AgCl was also observed (SI 1), consistent with an expected change in the ferrocene environment upon coupling.

The grafting of the phenylalanine moiety onto the ferrocene monolayer was further investigated by determination of the charge transfer resistance ($R_{ct}$) to diffusing ferricynide $Fe(CN)_6^{3-/4-}$ redox probe using electrochemical impedance spectroscopy (EIS). The $R_{ct}$ was seen to increase from $2.6\times10^5$ to $4.5\times10^5\ \Omega$ upon grafting of the phenylalanine (SI 2a). Only negligible changes in the $R_{ct}$ were seen when the ferrocene-modified electrode was immersed in amino-DL-phenylalanine without $NaNO_2$, confirming the diazonium-specific nature of chemical

coupling reaction. Further, $R_{ct}$ of the phenylalanine-terminated film was seen to increase suddenly when the pH was raised above pH = 9 (SI 2 b,c). This increased pH is associated with the deprotonation of the phenylalanine amine (pKa = 9.1) leading to a net negative charge on the film and increased repulsion of the $Fe(CN)_6^{3-/4-}$ redox probe. Hence, the increase in $R_{ct}$ at pH > 9 is a signature for presence of the phenylalanine film – as previously reported [13].

Contact angle measurements also supported the immobilisation of the phenylalanine. A large decrease in the water contact angle from (84 ± 3) to (42 ± 5)° was observed upon immersion of the ferrocene terminated layers in the amino-DL-phenylalanine/$NaNO_2$ solution – consistent with the grafting of the hydrophilic phenylalanine moiety onto the hydrophobic alkyl ferrocene terminated monolayer. No significant change in contact angle was observed when the reaction was carried out in the absence of $NaNO_2$ – with the contact angle remaining at (80 ± 5)° – further confirming a diazonium-specific chemical coupling reaction of the phenylalanine moiety.

The attachment of the phenylalanine moiety onto the ferrocene film was further probed by comparing protein adsorption onto the ferrocenethiol modified electrodes before and after grafting of the protein resistive [9] phenylalanine layer. Ferrocene modified electrodes (prior to attachment of phenylalanine) exhibited a decrease in the charge associated with $Fc/Fc^+$ redox couple to ~67 % of its initial value upon addition of 10 µM BSA to the electrolytic solution – consistent with fouling of the electrode due to BSA adsorption inhibiting electroactivity. In contrast > 95 % of the charge associated with $Fc/Fc^+$ redox couple remained when the same experiment was undertaken at the ferrocenephenylalanine modified electrode, indicating the expected antifouling properties of the phenylalanine layer (and supporting the successful coupling of antifouling phenylalanine to the ferrocene primer layer).

Following attachment of the relevant antibody (anti-BSA or anti-CRP) via peptide bond formation (Scheme 1, step 3) the surface concentration of electroactive ferrocene moieties was seen to further decrease to approximately $1.0 \times 10^{-10}$ mol cm$^{-2}$ and $0.5 \times 10^{-10}$ mol cm$^{-2}$ for the BSA and CRP receptive interfaces, respectively. This may be due to further passivation of the surface due to formation of the receptive antibody layer. Nevertheless, the remaining ferrocene signal proved sufficient for highly sensitive target detection. Changes in the water contact angle to (57 ± 5)°, and increase in $R_{ct}$ (SI 2a), further confirmed the success of the coupling reaction.

Following the construction of the sensing electrode interfaces, their suitability for the selective detection of specific proteins (BSA and CRP), was assessed. For both interfaces, increasing responses (i.e. decreases in $Fc/Fc^+$ charge) were observed upon immersion in increasing concentration of target protein between 10 pM and 10 nM.

The attenuation of the $Fc/Fc^+$ redox signal in the presence of target protein can be attributed to decreased solvent/electrolyte access, and/or a change in the local dielectric around the surface bound ferrocene, upon target binding [7b]. The response was seen to increase in a logarithmic fashion with increasing target concentration, in line with expectations. The resulting analytical curves are shown in Figure 2. The linear detection range between 10 pM and 10 nM facilitates measurements within the clinically useful range for CRP [14]. The limits of detection of 4.0 and 1.6 pM (0.265 and 0.192 ng/mL) for the BSA and CRP receptive interfaces, respectively, compare favourably with previous reports of label-free electrochemical CRP detection methodologies [6a, 7b, d] and show higher sensitivity than previously reported for traditional detection of CRP by ELISA (58 pM, 7 ng/mL) [15].

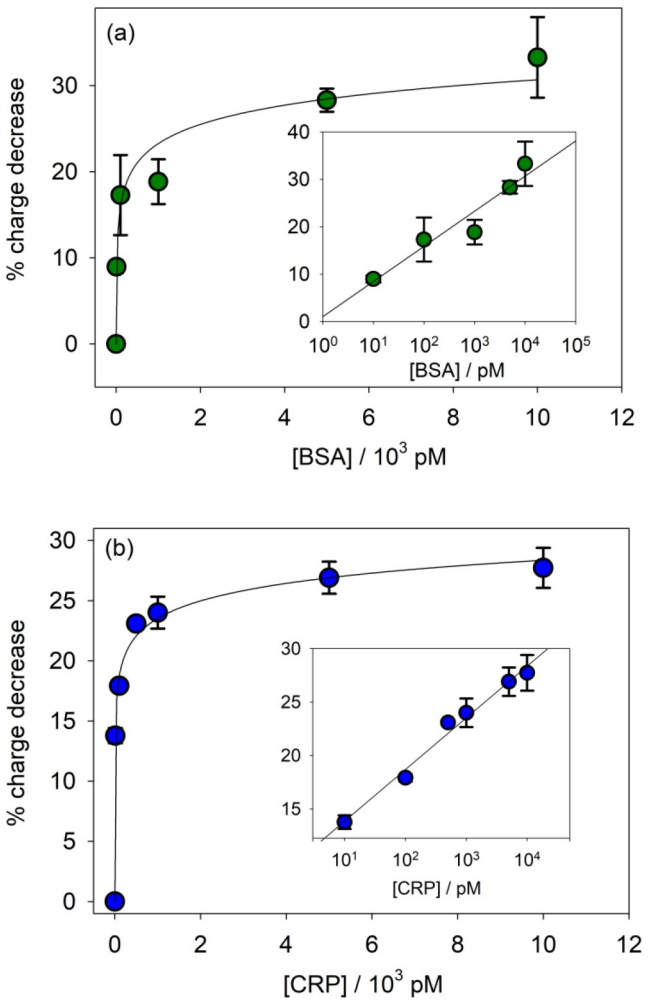


Fig. 2. Analytical curves reporting the percentage decrease in $Fc/Fc^+$ charge as a function of target concentration for both BSA (a) and CRP (b) receptive interfaces. $R^2$ (the coefficient of determination) for BSA is 0.981 and $R^2$ for CRP is 0.992. Inserts show the same analytical curves displayed with a logarithmic x-axis. Voltammograms shown in SI 3.

Selectivity of the sensing interfaces was explored by immersion of the pristine receptive sensing interfaces (prior to exposure to target protein) in 10 μM non-specific protein (RSA for the BSA receptive interfaces, and BSA for the CRP receptive interfaces) and human serum (20 %) in aqueous electrolyte. In all cases the sensor response to non-specific protein correlated to less than the LOD of the target protein (Figure 3) showing a high level of selectivity even at high concentration of non-specific protein. Despite the highly competitive LODs and selectivities observed, there is still considerable scope for future optimisation of the present approach.

Hence we have reported a simple, flexible, novel route to the fabrication of selective BSA and CRP receptive biosensing interfaces, enabling the label-free electrochemical quantification of these target proteins. The detection ranges and LODs for CRP fall within the clinically useful range for diagnosis of inflammation, cancer, and cardiovascular disease. Furthermore, this versatile sensing strategy should be translatable to many other protein biomarkers. Since low LODs compare well with those of ELISA (often in the low ng/mL and pM range) [16] the approach could underpin rapid and cost-effective diagnostics and prognostics of many conditions.

## *Experimental*

All electrochemistry was carried on a μ-autolab PGSTAT204 or PalmSens4 potentiostat using a three-electrode cell with an Ag/AgCl reference electrode, a platinum wire counter electrode, and a gold disk working electrode (BASi, $d = 1.6$ mm). The gold disk electrodes were prepared as previously reported [17]. The active area of the electrode was calculated by integrating the peak associated with the reduction of the gold oxide and comparing with the theoretical charge of 400 $\mu C\,cm^{-2}$ for an ideally flat gold electrode [18]. These electrochemically determined areas (0.026–0.030 $cm^2$) were used for determination of surface concentrations of ferrocene. EIS spectra were recorded in 2 mM $[Fe(CN)_6]^{3-/4-}$ in $NaClO_4$ or phosphate buffer. $R_{ct}$ values were determined by a fit to a Randles circuit. Water contact angle measurements were conducted on films of gold (100 nm) evaporated onto Si wafer substrates with a titanium binding layer.

The construction of the sensing interfaces is outlined in Scheme 1. Initially ferrocenethiol monolayers were formed by immersing the gold disk electrodes in a ~1 mM solution of 11-ferrocenylundecanethiol (Sigma-Aldrich) in ethanol for approximately 20 hours. Subsequently the phenylalanine film was coupled to the ferrocenethiol monolayer by immersing the modified electrodes in an aqueous solution containing 5 mM amino-DL-phenylalanine (Alfa Aesar) and 5 mM $NaNO_2$ in 0.5 M HCl. The antibody, anti-BSA (Sigma-Aldrich, B2901) or anti-CRP (Sigma-Aldrich, C1688), was coupled to the phenylalanine layer by activation of the terminal carboxylic acid group by immersion in an aqueous solution containing 0.1 M N-hydroxysuccinimide and 0.4 M 1-ethyl-3-(3-dimethylaminopropyl)carbodiimide for 40 min prior to immersion in a 5 μM solution of anti-CRP or anti-BSA in 0.01 M phosphate buffer (PB, pH 7.4) for 3 hours. The antibody-modified electrodes were immersed in a 5 mM solution of amino-DL-phenylalanine to deactivate any remaining activated carboxylic acid groups.

Assaying (sensor testing) was undertaken by recording cyclic voltammograms of the $Fc/Fc^+$ couple in PB (0.1 M, pH = 7.4) at a scan rate of 0.1 $Vs^{-1}$. Initially voltammograms were recorded in the absence of any protein (only PB). Controls were undertaken by immersing the electrodes in a 10 μM solution of non-specific protein in PB for 10 min prior to recording voltammograms. Subsequently assaying was carried out by immersing the sensing electrode in solutions of increasing concentration of target protein (1–10000 pM) in PB for 10 min and recording voltammograms. Immersion for longer than 10 min (up to 30 min) led to no significant change in voltammetric response at a certain target concentration.

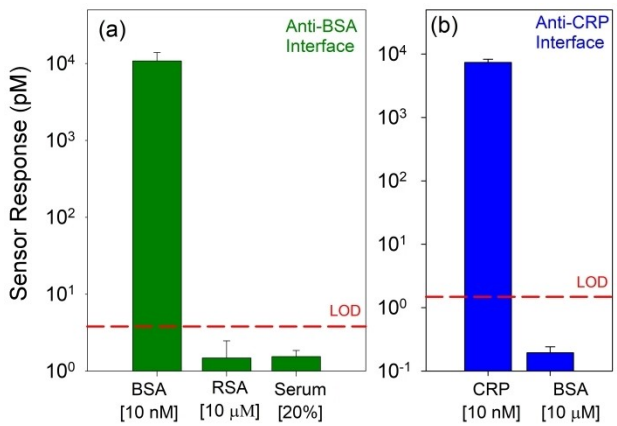


Fig. 3. Controls showing sensor response to specific protein (10 nM), non-specifc protein (10 μM), and human serum (20 %) – for BSA (a) and CRP (b) receptive surfaces.

## *Data Availability Statement*

The data that support the findings of this study are available from the corresponding author upon reasonable request.

## *References*

[1] a) S. B. Nimse, M. D. Sonawane, K.-S. Song, T. Kim, *Analyst* **2016**, *141*, 740–755; b) L. Wu, X. Qu, *Chem. Soc. Rev.* **2015**, *44*, 2963–2997.

[2] a) X. Fan, I. M. White, S. I. Shopova, H. Zhu, J. D. Suter, Y. Sun, *Anal. Chim. Acta* **2008**, *620*, 8–26; b) B. Špačková, P. Wrobel, M. Bocková, J. Homola, *Proc. IEEE* **2016**, *104*, 2380–2408.

[3] J. Tamayo, P. M. Kosaka, J. J. Ruz, Á. San Paulo, M. Calleja, *Chem. Soc. Rev.* **2013**, *42*, 1287–1311.

[4] N. J. Ronkainen, H. B. Halsall, W. R. Heineman, *Chem. Soc. Rev.* **2010**, *39*, 1747–1763.

[5] F. Lisdat, D. Schaefer, *Anal. Bioanal. Chem.* **2008**, *391*, 1555–1567.
[6] a) Q. Xu, H. Cheng, J. Lehr, A. V. Patil, J. J. Davis, *Anal. Chem.* **2015**, *87*, 346–350; b) C. Gautier, C. Esnault, C. Cougnon, J.-F. Pilard, N. Casse, B. Chénais, *J. Electroanal. Chem.* **2007**, *610*, 227–233; c) J. S. Daniels, N. Pourmand, *Electroanalysis* **2007**, *19*, 1239–1257.
[7] a) Y. Huang, Y. Ding, T. Li, M. Yang, *Anal. Methods* **2015**, *7*, 411–415; b) J. Lehr, F. C. Bedatty Fernandes, P. R. Bueno, J. J. Davis, *Anal. Chem.* **2014**, *86*, 2559–2564; c) W. Li, Z. Ma, *Sens. Actuators B* **2017**, *248*, 545–550; d) J. Piccoli, R. Hein, A. H. El-Sagheer, T. Brown, E. M. Cilli, P. R. Bueno, J. J. Davis, *Anal. Chem.* **2018**, *90*, 3005–3008.
[8] D. Hetemi, V. Noël, J. Pinson, *Biosensors* **2020**, *10*, 4.
[9] Q. Zou, L. L. Kegel, K. S. Booksh, *Anal. Chem.* **2015**, *87*, 2488–2494.
[10] L. Y. S. Lee, T. C. Sutherland, S. Rucareanu, R. B. Lennox, *Langmuir* **2006**, *22*, 4438–4444.
[11] a) S. Baranton, D. Bélanger, *J. Phys. Chem. B* **2005**, *109*, 24401–24410; b) D. Belanger, J. Pinson, *Chem. Soc. Rev.* **2011**, *40*, 3995–4048.
[12] N. Marshall, A. Rodriguez, S. Crittenden, *RSC Adv.* **2018**, *8*, 6690–6698.
[13] N. Menegazzo, Q. Zou, K. S. Booksh, *New J. Chem.* **2012**, *36*, 963–970.
[14] V. Vermeeren, L. Grieten, N. Vanden Bon, N. Bijnens, S. Wenmackers, S. D. Janssens, K. Haenen, P. Wagner, L. Michiels, *Sens. Actuators B* **2011**, *157*, 130–138.
[15] E. M. Macy, T. E. Hayes, R. P. Tracy, *Clin. Chem.* **1997**, *43*, 52–58.
[16] S. Zhang, A. Garcia-D′Angeli, J. P. Brennan, Q. Huo, *Analyst* **2014**, *139*, 439–445.
[17] J. Tkac, J. J. Davis, *J. Electroanal. Chem.* **2008**, *621*, 117–120.
[18] S. Trasatti, O. A. Petrii, *Pure Appl. Chem.* **1991**, *63*, 711–734.

Received: June 30, 2020
Accepted: January 5, 2021
Published online on ■■, ■■

  

# SHORT COMMUNICATION

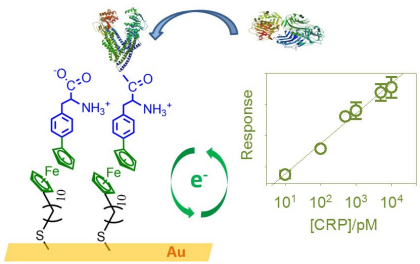


*C.-Y. Chen, J. Lehr**